

Optical emission of a molecular nanoantenna pair

E. M. Rice and D. L. Andrews

Citation: *J. Chem. Phys.* **136**, 244503 (2012); doi: 10.1063/1.4729784

View online: <http://dx.doi.org/10.1063/1.4729784>

View Table of Contents: <http://jcp.aip.org/resource/1/JCPSA6/v136/i24>

Published by the [American Institute of Physics](#).

Additional information on *J. Chem. Phys.*

Journal Homepage: <http://jcp.aip.org/>

Journal Information: http://jcp.aip.org/about/about_the_journal

Top downloads: http://jcp.aip.org/features/most_downloaded

Information for Authors: <http://jcp.aip.org/authors>

ADVERTISEMENT



ACCELERATE AMBER AND NAMD BY 5X.
TRY IT ON A FREE, REMOTELY-HOSTED CLUSTER.

LEARN MORE

Optical emission of a molecular nanoantenna pair

E. M. Rice and D. L. Andrews^{a)}

School of Chemistry, University of East Anglia, Norwich Research Park, Norwich NR4 7TJ, United Kingdom

(Received 1 March 2012; accepted 4 June 2012; published online 26 June 2012)

The optical emission from a pair of nanoantennas is investigated within the theoretical framework of quantum electrodynamics. The analysis of fluorescent emission from a pair of molecular antenna species in close proximity is prompted by experimental work on oriented semiconductor polymer nanostructures. Each physically different possibility for separation-dependent features in photon emission by any such pair is explored in detail, leading to the identification of three distinct mechanisms: emission from a pair-delocalized exciton state, emission that engages electrodynamic coupling through quantum interference, and correlated photon emission from the two components of the pair. Although each mechanism produces a damped oscillatory dependence on the pair separation, each of the corresponding results exhibits an analytically different form. Significant differences in the associated spatial frequencies enable an apparent ambiguity in the interpretation of experiments to be resolved. Other major differences are found in the requisite conditions, the associated selection rules, and the variation with angular disposition of the emitters, together offering grounds for experimental discrimination between the coupling mechanisms. The analysis paves the way for investigations of pair-wise coupling effects in the emission from nanoantenna arrays. © 2012 American Institute of Physics. [<http://dx.doi.org/10.1063/1.4729784>]

I. INTRODUCTION

It is well established that nanoscale variations in surface morphology can generate distinctive optical and electromagnetic effects, particularly in features that are associated with the excitation of plasmon resonances on metal surfaces. Along with the continued, burgeoning interest in such nano-optical properties, arising from an interplay of surface architecture and electronic structure, attention has recently begun to focus on other distinctive properties in nanoscale optics, such as those associated with a correlation, or quantum interference, between fluorescence from emitting sources positioned at closely separated surface sites.¹⁻⁴ Characteristic optical features are expected to become particularly prominent for emitters with a large oscillator strength (generally corresponding to a high magnitude transition dipole moment), as is the case with many of the nanoantenna systems studied in experiment. The coupling between antennas in close proximity is a subject of interest both for fundamental science,⁵⁻⁷ and with regard to many prospective applications. Prominent amongst the latter are devices for quantum information processing, sensing, and spectroscopy.⁸⁻¹⁰

The following study aims to secure a full understanding of the various mechanisms that can operate between electromagnetically coupled molecular antennas. This theoretical investigation has been prompted by important experimental work on pairs of oriented semiconducting polymer nanostructures—structures that exhibit a potential to act as effective room-temperature one-photon sources.¹¹ Barnes *et al.* devised an experiment to determine the coupling between two such nanoantennas by measuring fluorescence decay rates.¹² Using CN-PPV (cyano-substituted phenylene

vinylene) polymer, they found that the far-field decay rate of locally paired polymer nanostructures was significantly different from the emission of an isolated particle, exhibiting a distinctive damped oscillatory dependence on the pair separation—a feature reasonably interpreted as being due to coupling between the two centers. However, it proves possible to identify three physically quite different possibilities that might account for the emission characteristics of such a pair (Fig. 1). The initial interpretation has therefore left open a number of questions, such as the exact material parameters that determine the pair response in the reported measurements. This paper addresses the nature and characteristics of this and other potential coupling mechanisms, and their physical manifestations.

The paper is structured as follows. Section II introduces the formalism, based on quantum electrodynamics.^{13,14} Covering a wide range of phenomena, this is a framework singularly well suited to the identification of photonic interactions that occur on the nanoscale. An objective assessment of the pros and cons of such a representation, with respect to a semiclassical formulation, has recently been drawn out in a comprehensive volume by Grynberg *et al.*¹⁵ Continuing in Sec. III, detailed theory is developed for the three different possibilities of fluorescent emission by a pair of emitters; both the matter and the electromagnetic fields are treated quantum mechanically, and in each case the dependence on structure parameters and experimental variables is determined. In Sec. IV the results are compared to the experimental findings and conclusions of Barnes *et al.*, and set in a broader context. As well as resolving an ambiguity in the interpretation of mechanism for such experiments, our results will hopefully provide a stimulus for further experiments to ascertain and exploit various forms of electrodynamic coupling between antenna pairs.

^{a)}Electronic mail: david.andrews@physics.org.

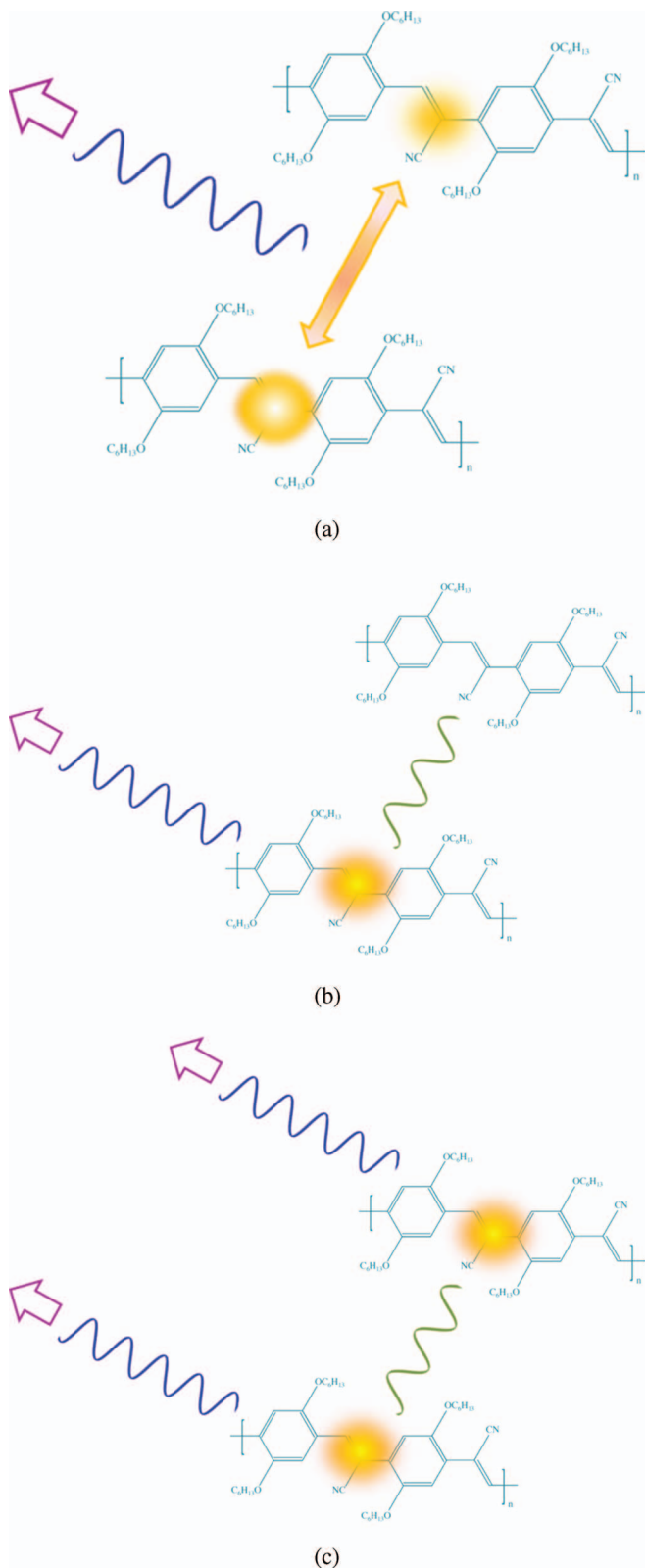


FIG. 1. Cartoon depictions of the possible mechanisms for separation-dependent emission by a pair of nanoantennas: (a) static coupling between the two centers supports a delocalized single excitation (the antisymmetric exciton state being illustrated) whose decay produces the emission of a single photon; (b) one electronically excited center emits under the dynamic influence of electromagnetic coupling with its neighbor; (c) the dynamically coupled pair is both electronically excited and emits two photons. In the figure, the antenna molecule CN-PPV used by Barnes *et al.* is shown by way of example.

II. QED BACKGROUND

A. System Hamiltonian

It is appropriate to begin with the generic quantum energy operator for a system comprising a number of antenna particles (molecules, chromophores, or quantum dots, for example) and the radiation field, described by multipolar coupling. This Hamiltonian is expressible as follows:

$$H = \sum_{\xi} H_{mat}(\xi) + \sum_{\xi} H_{int}(\xi) + H_{rad}, \quad (1)$$

where $H_{mat}(\xi)$ is the matter Hamiltonian of particle ξ , $H_{int}(\xi)$ signifies the interaction of that particle with the radiation field, and H_{rad} represents the radiation. The middle term describes interactions such as absorption and emission. The radiation field is present in vacuum fluctuations even when there is no observable light. In consequence, emission and absorption can entail not only “real” photons but also “virtual” photons, whose propagation between particles yields a state-perturbing influence.¹⁶ This means of interpreting inter-particle interactions is consistent with the retarded multipolar representation, where there is no term for direct coupling between antenna centers; it is a feature of this formulation that such interactions are mediated by the creation and annihilation of virtual photons.¹⁷

In the context of electronic excitation transfer, for example, it transpires that inter-particle phenomena traditionally classed as either “radiative” or “radiationless” transfer are not in fact separate mechanisms, but the short- and long-range asymptotes of a single unified coupling interaction.^{18,19} This observation is especially relevant for the following analysis. Energy transfer over nanoscale distances, beyond significant wavefunction overlap, generally entails a mechanism known as resonance energy transfer (RET), mainly associated with electric dipole-electric dipole (E1-E1) coupling. In this event, an excited donor emits excitation energy which is transferred to an acceptor; the donor falls back to its ground state while the acceptor is excited. In the QED theory this process is mediated by a virtual photon, coupling the donor decay and acceptor excitation through its creation and subsequent annihilation.²⁰

We shall be focusing on spontaneous emission processes, for which the relevant rate equations can be derived from time-dependent perturbation theory; in QED, spontaneous emission is understood to result from interaction of the excited system with the vacuum electromagnetic field.^{15,21} From Fermi’s Rule,²² the emission rate is given by

$$\Gamma = \frac{2\pi}{\hbar} |M_{fi}|^2 \rho_f, \quad (2)$$

where ρ_f is the density of final states, and the matrix element M_{fi} for the process follows from the standard perturbation expansion

$$M_{fi} = \langle f | H_{int} | i \rangle + \sum_{r \notin \{i, f\}} \frac{\langle f | H_{int} | r \rangle \langle r | H_{int} | i \rangle}{(E_i - E_r)} + \sum_{r, s \notin \{i, f\}} \frac{\langle f | H_{int} | s \rangle \langle s | H_{int} | r \rangle \langle r | H_{int} | i \rangle}{(E_i - E_s)(E_i - E_r)} + \dots \quad (3)$$

Here, $|i\rangle$ and $|f\rangle$ are the initial and final states of the system, $|r\rangle$ and $|s\rangle$ are intermediate states; E_j signifies the energy of state $|j\rangle$. In the electric dipole approximation the variation in electromagnetic fields over each particle is neglected, and the interaction Hamiltonian is

$$H_{int}(\xi) = -\frac{1}{\epsilon_0} \boldsymbol{\mu}^\xi \cdot \mathbf{d}^\perp(\mathbf{R}_\xi), \quad (4)$$

where $\boldsymbol{\mu}^\xi$ is the electric dipole moment operator of particle ξ positioned at the molecular origin \mathbf{R}_ξ (usually identified with the center of mass), and $\mathbf{d}^\perp(\mathbf{R}_\xi)$ is the operator for the transverse electric displacement field at that site.

B. Single-site fluorescence

To illustrate the methods to be used in the calculations below, we first consider a system comprising a single electronically excited antenna, decaying to its ground state by fluorescent emission. This introduction will deliver a result allowing later comparison with the effects of pair-wise coupling. Fluctuations in the quantized vacuum field perturb electronic motions so that the antenna excited state is no longer a stationary state of the system, allowing decay transition to occur; the loss of excitation energy appears as a photon added to the field.²³

To implement the dipolar coupling operator (4), we use the following quantum field expansion of \mathbf{d}^\perp over a complete set of radiation modes (\mathbf{k}, η) :

$$\begin{aligned} \mathbf{d}^\perp(\mathbf{r}) = i \sum_{\mathbf{k}, \eta} \left(\frac{\hbar c k \epsilon_0}{2V} \right)^{1/2} \{ e^{(\eta)}(\mathbf{k}) a^{(\eta)}(\mathbf{k}) e^{i\mathbf{k} \cdot \mathbf{r}} \\ - \bar{e}^{(\eta)} a^{\dagger(\eta)}(\mathbf{k}) e^{-i\mathbf{k} \cdot \mathbf{r}} \}. \end{aligned} \quad (5)$$

Here, $e^{(\eta)}(\mathbf{k})$ is the polarization vector of a radiation mode with wave-vector \mathbf{k} and polarization η , and $a^{(\eta)}(\mathbf{k})$, $a^{\dagger(\eta)}(\mathbf{k})$ are the corresponding photon annihilation and creation operators; V is an arbitrary quantization volume. Also in Eq. (5) and below, an over-bar is deployed to represent complex conjugation, so that the second term in (5) is the Hermitian conjugate of the first. Generally, the polarization vector is considered a complex quantity in order to accommodate circular polarizations. Since the annihilation and creation operators appear linearly in the field (5), it follows from (3) and (4) that the n th term in the perturbation series is the leading non-zero term for any mechanism that entails n photons (real and/or virtual). By standard methods it thus emerges that the spatially integrated rate of single-photon emission from an isolated particle is given by¹³

$$\Gamma_0 = \frac{k^3}{3\epsilon_0\pi\hbar} |\boldsymbol{\mu}^{0m}|^2, \quad (6)$$

where $k = (E_m - E_0)/\hbar c$ is the wave-number for the emission at circular frequency $\omega = ck$, produced by the electronic transition $0 \leftarrow m$, and $\boldsymbol{\mu}^{0m}$ is the associated electric dipole transition moment. The density of vibrational levels in large molecules or polymers is responsible for a broad linewidth in the electronic transition; their stochastic character serves to ensure that the usual Born-Oppenheimer separation of nuclear and electronic motions is a valid representation for the processes of interest. Equation (6) will be used as a reference

for the rates of emission by a pair, whose coupling produces modulations to this emission rate.

III. EMISSION BY A PAIR

A. Context

Barnes *et al.*¹² measured the fluorescence decay rate of a “probe” particle, an oriented CN-PPV nanostructure, in the presence of a second, chemically identical such particle, the pair being separated by distances from 200 nm to 2 μm . Enhancement and suppression of the decay (relative to an isolated particle) were observed at different distances, and the damped oscillatory dependence on displacement led to a deduction that dipole-dipole coupling was present. Citing work by Craig and Thirunamachandran,²⁴ there was a conclusion that this modification of decay rate arose as a result of vacuum modifications of the electromagnetic field associated with one dipole emitter, in the vicinity of the second, coherently radiating dipole. The perturbed decay rate, relative to the free space decay rate, was expressed as

$$\frac{\Gamma}{\Gamma_0} = 1 + \frac{3}{2} \text{Im}\{\boldsymbol{\mu}^{0m} \cdot \mathbf{E}\}, \quad (7)$$

\mathbf{E} designating a retarded electric field which, at a displacement \mathbf{R} from the second source, is duly expressible as^{16,25}

$$\begin{aligned} \mathbf{E} = \frac{e^{ikR}}{4\pi\epsilon_0 R^3} \{ [3(\boldsymbol{\mu}^{0m} \cdot \hat{\mathbf{R}})\hat{\mathbf{R}} - \boldsymbol{\mu}^{0m}] (1 - ikR) \\ + \{ \boldsymbol{\mu}^{0m} - (\boldsymbol{\mu}^{0m} \cdot \hat{\mathbf{R}})\hat{\mathbf{R}} \} k^2 R^2 \}. \end{aligned} \quad (8)$$

Here, $\mathbf{R} \equiv R\hat{\mathbf{R}}$ serves to define the magnitude and unit vector of the vector displacement from the molecular origin, and $\hbar\omega = \hbar ck$ is the energy of the photon emitted in $0 \leftarrow m$ decay.

Although the result cast in the form of Eq. (7) proved a reasonable fit to the experimental data, it is not in fact a formula delivered by the cited Craig and Thirunamachandran’s analysis—whose mechanism for the influence of intermolecular coupling on spontaneous emission explicitly depends on molecular polarizability. Accordingly, to make sense of the reported observations and to give a lead for further studies, it is our aim to explore in detail a wider range of mechanisms that might operate to produce such observations from an identical pair of emitters. As explained earlier, and as shown in Fig. 1, there are three distinct possibilities: (a) one photon is emitted from a pair of particles that together accommodate a single excitation, no prior measurement having localized excitation on either individual particle; (b) a photon is released by a pair for which prior measurement has established residence of the excitation on one specific component, the emission being subject to the influence of the neighboring particle; (c) two photons are emitted from a pair in which both particles are initially excited. In each case, electromagnetic coupling

between the two particles can be entertained, and its effects on features of the observed emission determined.

B. Three mechanisms for pair decay

1. One-photon emission from a pair with delocalized excitation

We first consider the situation that one of the two identical particles is electronically excited, leading to the emission of a single photon from the observed system. It is assumed that no prior measurement has localized excitation on either individual particle; the case is consistent with the establishment of a steady-state delocalized exciton, without measurement effecting wave-packet collapse at either center. The initial state of the system is therefore given by one of the

following combination states, i.e., symmetric and antisymmetric combinations:²⁶

$$|i\rangle = \frac{1}{\sqrt{2}} \{ |E_m^A, E_0^B; 0\rangle \pm |E_0^A, E_m^B; 0\rangle \}. \quad (9)$$

Here, E_p^ξ designates the energy of particle ξ in a state p , and the sequence in each ket designates the state of A , then B ; finally that of the radiation field. In the final state following emission, both particles are in their ground states and one photon is present,

$$|f\rangle = |E_0^A, E_0^B; 1(\mathbf{k}, \eta)\rangle. \quad (10)$$

In consequence the matrix element for the emission process is cast as follows, where the position of A arbitrarily defines the origin, and B is positioned at \mathbf{R} :

$$\begin{aligned} M_{fi}^\pm &= \frac{1}{\sqrt{2}} (M_{fi}^{(a)} \pm M_{fi}^{(b)}) \\ &\equiv \frac{1}{\sqrt{2}} \{ \langle 1(\mathbf{k}, \eta); E_0^B, E_0^A | -\varepsilon_0^{-1} \boldsymbol{\mu}^A \cdot \mathbf{d}^\perp(\mathbf{0}) - \varepsilon_0^{-1} \boldsymbol{\mu}^B \cdot \mathbf{d}^\perp(\mathbf{R}) | E_m^A, E_0^B; 0 \rangle \\ &\quad \pm \langle 1(\mathbf{k}, \eta); E_0^B, E_0^A | -\varepsilon_0^{-1} \boldsymbol{\mu}^A \cdot \mathbf{d}^\perp(\mathbf{0}) - \varepsilon_0^{-1} \boldsymbol{\mu}^B \cdot \mathbf{d}^\perp(\mathbf{R}) | E_0^A, E_m^B; 0 \rangle \} \\ &= \frac{1}{\sqrt{2}} \varepsilon_0^{-1} \{ -\langle E_0^A | \boldsymbol{\mu}^A | E_m^A \rangle \cdot \langle 1(\mathbf{k}, \eta) | \mathbf{d}^\perp(\mathbf{0}) | 0 \rangle \mp \langle E_0^B | \boldsymbol{\mu}^B | E_m^B \rangle \cdot \langle 1(\mathbf{k}, \eta) | \mathbf{d}^\perp(\mathbf{R}) | 0 \rangle \}. \end{aligned} \quad (11)$$

Other parameters are defined in Fig. 2, exhibiting the time-ordered diagram for the process.

Using the explicit form of the transverse electric displacement field operator from (5), deploying the electric dipole approximation, and using the convention of implied summation over repeated indices (the latter denoting Cartesian components), the matrix element for emission into a specific radiation mode reduces to

$$M_{fi}^\pm = -\frac{i}{\sqrt{2}} \left(\frac{\hbar ck}{2\varepsilon_0 V} \right)^{1/2} \mu_i^{0m} \bar{e}_i^{(\eta)} [1 \pm e^{-i\mathbf{k}\cdot\mathbf{R}}] \quad (12)$$

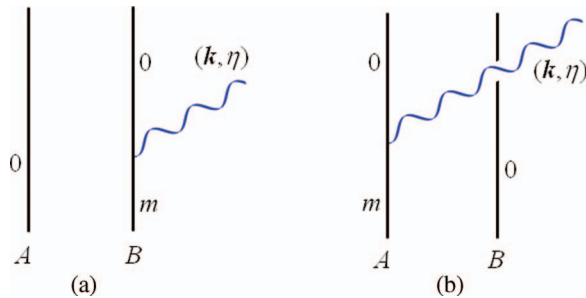


FIG. 2. The time-ordered diagrams for photon emission by one excited particle in the vicinity of another in its ground state, time progressing upwards: m represents the excited state and 0 the ground state; \mathbf{k} is the wave-vector for the emitted photon and η denotes the corresponding polarization.

on the simplifying assumption that the transition dipole moments of A and B have a common magnitude and orientation. For two emitters that are very close together, where $\mathbf{k} \cdot \mathbf{R} \sim 1$, the result leads to the familiar pair of radiating and non-radiating states. More generally, from Fermi's rule (2), the rate of emission is proportional to

$$|M_{fi}^\pm|^2 = \frac{1}{2} \left(\frac{\hbar ck}{2\varepsilon_0 V} \right) \mu_i^{0m} \bar{\mu}_j^{0m} \bar{e}_i^{(\eta)} e_j^{(\eta)} [2 \pm e^{i\mathbf{k}\cdot\mathbf{R}} \pm e^{-i\mathbf{k}\cdot\mathbf{R}}]. \quad (13)$$

If the emission is not resolved for any particular polarization, it is necessary to sum over both polarizations η of any suitable basis set (e.g., left- and right-handed, or two orthogonal linear polarizations), which can be achieved using the relation,¹³

$$\sum_{\eta} e_i^{(\eta)}(\mathbf{k}) \bar{e}_j^{(\eta)}(\mathbf{k}) = \delta_{ij} - \hat{k}_i \hat{k}_j \quad (14)$$

effecting the necessary tensor and vector contractions in Eq. (13). To secure the overall emission rate, the resulting expression now needs to be integrated over all directions of the wave-vector \mathbf{k} with respect to \mathbf{R} and each μ^{0m} ; we assume the latter are real-valued. The term without a phase factor is straightforward, and the solid angle integral of (14) delivers $(8\pi/3)\delta_{ij}$. The remaining, phase-bearing terms in (13) each give a factor of $4\pi\varepsilon_0 k^{-3} \tau_{ij}$ in which τ_{ij} is the imaginary part of a retarded coupling tensor that will arise in Sec. III B, and

is defined by²⁷

$$\begin{aligned}\tau_{ij}(k, \mathbf{R}) &= \frac{k_3}{4\pi\epsilon_0} \int (\delta_{ij} - \hat{k}_i\hat{k}_j) e^{\pm ik\cdot\mathbf{R}} d\Omega \\ &= \frac{1}{4\pi\epsilon_0 R^3} [(\delta_{ij} - 3\hat{R}_i\hat{R}_j)(\sin kR - kR \cos kR) \\ &\quad - (\delta_{ij} - \hat{R}_i\hat{R}_j)k^2 R^2 \sin kR] \quad (15)\end{aligned}$$

(see also Ref. 31). Making the appropriate substitutions in (13) gives

$$|M_{fi}^\pm|^2 = \left(\frac{\hbar ck}{2\epsilon_0 V}\right) \left[\frac{8\pi}{3} (\mu^{0m})^2 \pm 4\pi\epsilon_0 k^{-3} \mu_i^A \mu_j^B \tau_{ij}(kR) \right] \quad (16)$$

and the rate of emission follows from Eq. (2),

$$\Gamma^\pm = \left(\frac{k^3}{6\pi\epsilon_0\hbar}\right) \left[2(\mu^{0m})^2 \pm \frac{\epsilon_0\mu_i\mu_j\tau_{ij}(kR)}{k^3} \right], \quad (17)$$

using the formula²⁸ $\rho_f = k^2 V / 8\pi^3 \hbar c$ for the density of final states (the number of radiation states per unit energy interval) per unit solid angle. Explicitly, we then have

$$\begin{aligned}\Gamma^\pm &= \left(\frac{k^3}{6\pi\epsilon_0\hbar}\right) \left[2(\mu^{0m})^2 \pm \mu_i\mu_j \frac{1}{4\pi k^3 R^3} \right. \\ &\quad \times \{(\delta_{ij} - 3\hat{R}_i\hat{R}_j)(\sin kR - kR \cos kR) \\ &\quad \left. - (\delta_{ij} - 3\hat{R}_i\hat{R}_j)k^2 R^2 \sin kR\} \right]. \quad (18)\end{aligned}$$

In the near-zone, the leading term in the result is the one with the largest inverse power of kR . With a Taylor series expansion of the sin function, the distance-dependent contribution to the rate emerges with an angle- and distance-dependence determined by $\pm(kR)^{-2}(|\mu^{0m}|^2 - 3|\mu^{0m} \cdot \hat{\mathbf{R}}|^2)$. However, our main interest lies in the asymptotic form of result for the $kR \gg 1$ regime, where a damped oscillatory dependence on pair separation is anticipated. Here, the distance-dependent rate contribution is dominated by the last term in (18), running as $\pm(kR)^{-1} \sin kR (|\mu^{0m}|^2 - |\mu^{0m} \cdot \hat{\mathbf{R}}|^2)$. A notable, if unusual, exception would be a case where both transition dipoles are aligned parallel to the displacement vector \mathbf{R} , as might arise with nanoemitters lying along a surface to which both adhere. In such an instance the final term in (18) vanishes and the result is largely controlled by a $\pm(kR)^{-2} \cos kR$ dependence.

Now from Eq. (8), it follows that $\text{Im}\{\mu^A \cdot \mathbf{E}\}$ is none other than $\mu_i\mu_j\tau_{ij}$ cast in the form of implied index summation; this factor is associated with a damped, strongly oscillatory behavior with respect to the pair separation R . Comparing the rate of pair emission (17) with the corresponding expression for an isolated molecule, Eq. (6), thus reveals in the case of a symmetric exciton (positive sign in the above result) a rate ratio exactly as represented in (7), the result given by Barnes *et al.*, and a result which suitably fits their data.¹² Notice that explicit coupling of the two emitters is not involved; the characteristic rate modification only exhibits the fact that their single excitation is delocalized between the pair.

It is also worth observing that if the symmetric and antisymmetric exciton states become degenerate, then in general one should add the results for the two cases—and their contributions to this interference mechanism then exactly cancel. Accordingly, observations of an emission rate with a damped oscillatory dependence on the pair separation, due to this interference mechanism, require a sufficient lifting of degeneracy that only one of the exciton states is initially excited.

Explicit electrodynamic coupling between the two emitters in fact introduces a second mechanism, to be examined in Sec. III B 2. It is the following mechanism that one can identify physically with the modification of the vacuum electromagnetic field associated with one dipole emitter, in the vicinity of the second, fitting the description (but not the analytical mechanism) described by Barnes *et al.*

2. One-photon emission from a pair with localized excitation

In the second case to be examined, emission from a specifically excited particle A takes place under conditions that are electrodynamically tempered by coupling to B , the latter assumed to be non-polar. The initial and final states are: $|i\rangle = |E_m^A, E_0^B; 0\rangle$; $|f\rangle = |E_0^A, E_0^B; 1(\mathbf{k}, \eta)\rangle$, and the leading contribution to the matrix element is the following term, from first-order perturbation theory:

$$M_{fi}^{(1)} = -i \sum_{\mathbf{k}, \eta} \left(\frac{\hbar ck}{2\epsilon_0 V}\right)^{1/2} \mu_i^{0m} \bar{e}_i^{(\eta)} \quad (19)$$

signifying independent emission by A (the phase factor is unity since A is sited at the origin).

As noted earlier, coupling between particles can be mediated only by pair-wise interactions with the radiation field, and accordingly accommodates virtual photon transfer. There are six possible time-orderings for this process (Fig. 3), and the matrix element is calculated taking each of these into account. This follows the usual rule that requires the addition of quantum amplitudes connecting the same initial and final states. Since three photon interactions feature in this process (the creation and annihilation of the virtual photon as well as emission of a real photon), third order perturbation theory is used—the third term in (3). The matrix element found by summing over intermediate states corresponds to the mechanism considered by Craig and Thirunamachandran. From the time-ordering represented by the graph in Fig. 3(a), for example, with intermediate states $|r\rangle = |E_0^A, E_0^B; 1(\mathbf{p}, \eta)\rangle$; $|s\rangle = |E_0^A, E_n^B; 0\rangle$, we have²⁴

$$\begin{aligned}M_{fi}^{(3)a} &= -i \sum_{\mathbf{p}, r, \eta, \eta'} \left(\frac{\hbar ck}{2\epsilon_0 V}\right)^{1/2} \left(\frac{\hbar cp}{2\epsilon_0 V}\right) \\ &\quad \times \bar{e}_i^{(\eta)}(\mathbf{p}) e_j^{(\eta')}(\mathbf{p}) \bar{e}_k^{(\eta)}(\mathbf{k}) \mu_i^{0m}(A) \mu_j^{r0}(B) \mu_k^{0r}(B) e^{i\mathbf{p}\cdot\mathbf{R}} e^{-i\mathbf{k}\cdot\mathbf{R}} \\ &\quad \times \frac{1}{(E_{m0}^A - E_{r0}^B)(E_{m0}^A - \hbar cp)}, \quad (20)\end{aligned}$$

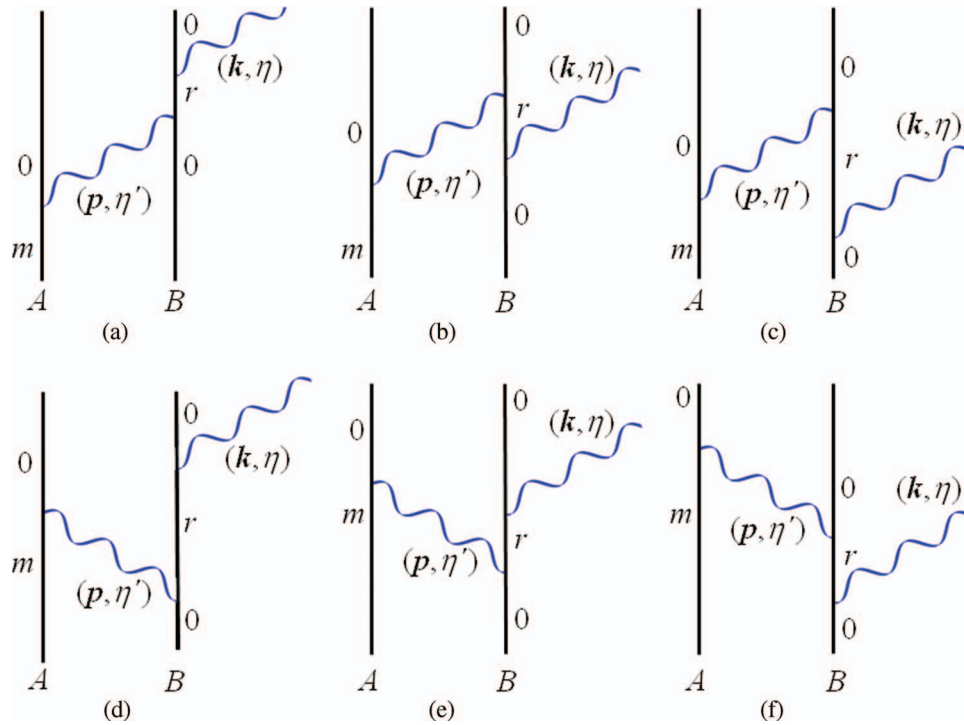


FIG. 3. The six time-ordered diagrams for photon emission from B with electrodynamic coupling to the electronic decay of A ; \mathbf{p} is the wave-vector of a virtual photon and η' its polarization; r is a virtual intermediate state. A further six graphs, conveying emission from A with static coupling between A and B , would arise if the latter were polar, i.e., if it had a static electric dipole moment.

where $E_{m0} = E_m - E_0 \equiv \hbar ck$. With a similar analysis of all six graphs in Fig. 3, summation of the corresponding contributions now gives

$$M_{fi}^{(3)} = -i \sum_{\mathbf{p}, \eta, \eta'} \left(\frac{\hbar ck}{2\epsilon_0 V} \right)^{1/2} \left(\frac{\hbar c \mathbf{p}}{2\epsilon_0 V} \right) \bar{e}_i^{(\eta')}(\mathbf{p}) e_j^{(\eta)}(\mathbf{p}) \bar{e}_k^{(\eta)}(\mathbf{k}) e^{-i\mathbf{k} \cdot \mathbf{R}} \times \left\{ \frac{e^{i\mathbf{p} \cdot \mathbf{R}}}{(\hbar c \mathbf{p} - E_{m0}^A)} + \frac{e^{-i\mathbf{p} \cdot \mathbf{R}}}{(\hbar c \mathbf{p} + E_{m0}^A)} \right\} \mu_i^{0m}(A) \alpha_{jk}^B(\omega), \quad (21)$$

where $\omega = ck$ and the dynamic polarizability α_{ij} of B is given by the usual formula

$$\alpha_{ij}(\omega) = \sum_r \left[\frac{\mu_i^{0r} \mu_j^{r0}}{E_{r0} + \hbar\omega} + \frac{\mu_j^{0r} \mu_i^{r0}}{E_{r0} - \hbar\omega} \right] \equiv \frac{2}{\hbar} \sum_r \mu_i^{r0} \mu_j^{r0} \left[\frac{\omega_{r0}}{\omega_{r0}^2 - \omega^2} \right] \quad (22)$$

and the second equality, based on the assumption of real transition moments, delivers the polarizability in its most familiar text-book form.

Proceeding with the mode integration and vector calculus as shown in the Appendix, we secure a result (A7) that is succinctly expressible as

$$M_{fi}^{(3)} = -i \left(\frac{\hbar ck}{2\epsilon_0 V} \right)^{1/2} \bar{e}_k^{(\eta)}(\mathbf{k}) e^{-i\mathbf{k} \cdot \mathbf{R}} \mu_i^{0m}(A) \alpha_{jk}^B(\omega) V_{ij}(k, \mathbf{R}), \quad (23)$$

where $V_{ij}(kR)$ is the standard E1-E1 retarded coupling tensor, given by^{29,30}

$$V_{ij} = \frac{e^{i\mathbf{k} \cdot \mathbf{R}}}{4\pi\epsilon_0 R^3} [(\delta_{ij} - 3\hat{R}_i \hat{R}_j) - (i\mathbf{k}R)(\delta_{ij} - 3\hat{R}_i \hat{R}_j) - k^2 R^2 (\delta_{ij} - \hat{R}_i \hat{R}_j)]. \quad (24)$$

In passing we note the link with the retarded field in (8), namely, $E_j = -\mu_i V_{ij}$; moreover, $\text{Im}\{V_{ij}\} = \tau_{ij}$. A clear physical interpretation of the result (23) thus becomes apparent; it is the quantum amplitude for the emergence of a photon from the decay of A , after scattering by B ; that is why the polarizability of B is entailed. However, the result clearly incorporates time-sequences other than that which corresponds to Fig. 3(a), reflecting the significance of time-energy uncertainty within the frame of measurement.

The calculation now requires squaring the modulus of the total matrix element and averaging over all directions of \mathbf{k} , then finding the rotational average over all $\boldsymbol{\mu}$ with respect to \mathbf{R} . Substituting the result into Fermi's rule (2) we have

$$\Gamma = \frac{2\pi}{\hbar} |M_{fi}^{(1)} + M_{fi}^{(3)} + \dots|^2 \rho_f = \frac{2\pi\rho_f}{\hbar} \{ |M_{fi}^{(1)}|^2 + 2\text{Re} \bar{M}_{fi}^{(1)} M_{fi}^{(3)} + \dots \}. \quad (25)$$

Deploying the density of states for the radiation, the position-independent first term on the right leads to the familiar isotropically averaged result

$$\Gamma^{(1,1)} = \left(\frac{k^3}{3\pi\epsilon_0 \hbar} \right) (\mu^{0m})^2. \quad (26)$$

To identify any dependence on the pair separation, our attention duly turns to the leading interference term. First,

summing over emission modes again using the density of radiation states, assuming A and B have a common orientation, Eqs. (19), (23), and (25) give

$$\Gamma^{(1,3)} = \text{Re} \left(\frac{k^3}{4\pi^2 \hbar} \right) \mu_l^{0m} e_l^{(\eta)} \mu_i^{0m} V_{ij}(k, \mathbf{R}) \alpha_{jk} \bar{e}_k^{(\eta)} e^{-ik \cdot \mathbf{R}}. \quad (27)$$

Following the standard sum over polarizations, Eq. (14), the average over emission directions is required. It is not

straightforward to tackle the associated rotational average; considerable complexity arises in the term that bears a phase-weighted second rank tensor engagement between components of the wave-vector and the electrodynamic properties of the pair. However, an exact analytical procedure has been established for such calculations;³¹ the results necessary for the present calculation are drawn from the general analysis and cast in terms of spherical Bessel functions j_n . Specifically, we have

$$\langle e^{-ik \cdot \mathbf{R}} \rangle = j_0(-kR) = (kR)^{-1} \sin kR, \quad (28)$$

$$\begin{aligned} \langle P_{kl} \hat{k}_k \hat{k}_l e^{-ik \cdot \mathbf{R}} \rangle &= \frac{1}{3} j_0(-kR) P_{kk} - \frac{3}{2} j_2(-kR) \left(1 - \frac{1}{3}\right) \left(P_{kl} \hat{R}_k \hat{R}_l - \frac{1}{3} P_{kk}\right) \\ &= \frac{1}{3} (kR)^{-1} P_{kk} \sin kR + \left[\left(\frac{1}{kR} - \frac{3}{(kR)^3} \right) \sin kR + \frac{3}{(kR)^2} \cos kR \right] \left(P_{kl} \hat{R}_k \hat{R}_l - \frac{1}{3} P_{kk} \right), \end{aligned} \quad (29)$$

where for shorthand we signify the transition moment coupling by

$$P_{kl} = \mu_i^{0m} V_{ij}(k, \mathbf{R}) \alpha_{jk} \mu_l^{0m}. \quad (30)$$

Thus, from Eqs. (27)–(29), we obtain

$$\Gamma^{(1,3)} = \text{Re} \left(\frac{1}{4\pi^2 \hbar R^3} \right) [3 \sin kR - 3kR \cos kR - k^2 R^2 \sin kR] \left(P_{kl} \hat{R}_k \hat{R}_l - \frac{1}{3} P_{kk} \right). \quad (31)$$

Now from (24), (30), and (31), we finally secure the rate

$$\begin{aligned} \Gamma^{(1,3)} &= \left(\frac{1}{48\pi^3 \hbar \epsilon_0 R^6} \right) [3 \sin kR - 3kR \cos kR - k^2 R^2 \sin kR] \\ &\quad \times [\mu_i^{0m} \alpha_{ik} \mu_l^{0m} \hat{R}_k \hat{R}_l (6 \cos kR + 6kR \sin kR - 4k^2 R^2 \cos kR) \\ &\quad - 3\mu_i^{0m} \alpha_{jk} \mu_l^{0m} \hat{R}_i \hat{R}_j \hat{R}_k \hat{R}_l (3 \cos kR + 3kR \sin kR - k^2 R^2 \cos kR) \\ &\quad - \mu_i^{0m} \alpha_{ik} \mu_k^{0m} (\cos kR + kR \sin kR - k^2 R^2 \cos kR)], \end{aligned} \quad (32)$$

where use has been made of the result $\mu_i^{0m} \alpha_{ik} \mu_l^{0m} \hat{R}_k \hat{R}_l = \mu_i^{0m} \alpha_{jk} \mu_k^{0m} \hat{R}_i \hat{R}_j$, which follows by index substitution, recognizing the symmetry of the polarizability with respect to interchange of its indices. Notice that the terms where $\hat{\mathbf{R}}$ components appear vanish if the transition dipoles are perpendicular to the pair separation vector (oriented along a surface normal, for example), by virtue of the associated index contractions.

In contrast to the earlier investigation,²⁴ which took isotropic averages and focused on the regime $kR = 1$, we draw from our more general analysis the term that dominates the result for distances over the scale $kR \gg 1$, signifying pair separations up to and beyond one wavelength of the emitted radiation, as in the reports by Barnes *et al.*—and which also most effectively drives the oscillatory distance dependence. The emergent result is thus

$$\begin{aligned} \Gamma^{(1,3)} &= \left(\frac{k^4}{96\pi^3 \hbar \epsilon_0 R^2} \right) \mu_i^{0m} [4\alpha_{ik} \mu_l^{0m} \hat{R}_k \hat{R}_l \\ &\quad - 3\alpha_{jk} \mu_l^{0m} \hat{R}_i \hat{R}_j \hat{R}_k \hat{R}_l - \alpha_{ik} \mu_k^{0m}] \sin 2kR. \end{aligned} \quad (33)$$

We shall return to this equation to discuss it in the context of the results for other mechanisms, in Sec. IV. Of course, although Eq. (33) is the leading term that involves both emitters, the next terms of higher order (such as $\Gamma^{(3,3)}$ and $\Gamma^{(1,5)}$) may play a part, though their contributions are expected to be negligible. Berman has, for example, shown that rescattering, whose quantum amplitude $M_{fi}^{(5)}$ interferes with $M_{fi}^{(1)}$ in generating $\Gamma^{(1,5)}$, should for consistency be included in calculations on two-atom spontaneous emission and scattering.³²

3. Correlated two-photon emission from a dually excited pair

A third, intriguing possibility arises when the particle pair has sufficient electronic energy for the excited state decay to release *two* photons. If this total energy were to be located on just one particle, the associated probability of two-photon emission might be considered negligible compared with single-photon absorption—although a recent report of

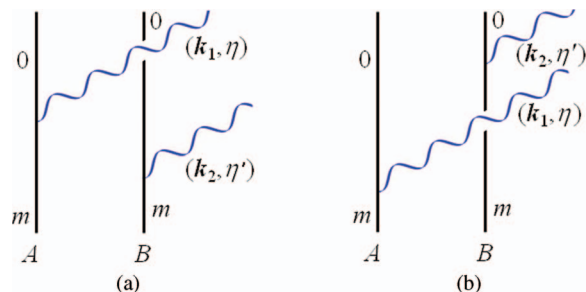


FIG. 4. Two time-ordered diagrams for two photon emission from the pair without coupling.

work on quantum dots has shown that such behavior is not out of the question.³³ However, any such emission involving a coupling between emitters would certainly be associated with much smaller probabilities than the other mechanisms under scrutiny. Here, we focus on the case where both particles are initially excited to the same quantum level, with the release of two photons signifying correlated emission from the pair.

Before proceeding further, it is useful to estimate the likelihood of the initial, dual excitation condition being satisfied by optical input. This can be gauged by the probability that, when one of the emitters is excited, the other will capture a photon during the decay lifetime of the first. The achievement of a suitably high probability is signified by a condition that is concisely expressible as $I\sigma\tau > \hbar\omega$, where I is the irradiance, σ is the absorption cross section, τ is the emissive decay lifetime and the quantity on the right is the incident photon energy. We have found no experimental studies that report the data enabling the quantity on the left to be evaluated, but, for example, with an irradiance of 10^{10} W m^{-2} , an absorption cross section 10^{-19} m^2 , a lifetime of 10^{-8} s , and a photon energy in the visible range, it is clear that the condition is easily satisfied, in this case in fact by around three orders of magnitude.

We begin by noting that the two time-orderings for the correlated emission of two photons from a dually excited but uncoupled pair, shown in Fig. 4, give equal and opposite matrix element contributions that exactly cancel out. Indeed, any such emission by the dually excited pair, whether correlated or independent, cannot give a result that carries the sought dependence on the pair separation. To secure a non-zero matrix element and corresponding rate of emission, and to secure a mechanism for dependence on the pair separation, it is again necessary that electromagnetic coupling occurs between the two emitters. The two emitted photons need not have precisely the same energy, and certainly not the same direction of emission; it suffices that their sum energy equals the energy initially possessed by the pair. For this reason we shall calculate the rate of emission of two photons in generally different modes (\mathbf{k}_1, η_1) , (\mathbf{k}_2, η_2) , with energy conservation requiring $\hbar c k_1 + \hbar c k_2 = 2\hbar c k \equiv 2E_{m0}$.

With four photon interactions (two real photon emissions, together with the creation and annihilation of a virtual photon), fourth order perturbation theory is the lowest order that can be deployed to give a non-vanishing result. The couplings

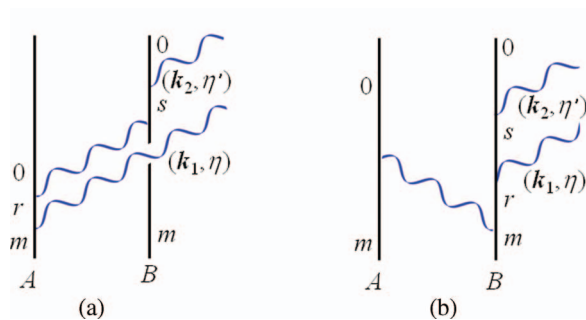


FIG. 5. Two representative time-ordered diagrams for two-photon emission from an electro-dynamically coupled pair; r and s are virtual intermediate states and the virtual photon labeling is suppressed. There are two types of mechanism with different selection rules: (a) the (2, 2) mechanism, illustrating one of 24 different time orderings; (b) the (1, 3) mechanism, again one of 24 orderings. In this case a further 24 diagrams arise on exchanging A and B , signifying the (3, 1) mechanism.

naturally fall into two distinct sets, examples of which are shown in Fig. 5. In Fig. 5(a) each particle has two interactions, a class which we represent by the shorthand notation (2, 2); in the second case, Fig. 5(b), one particle has a single interaction and the other has three, corresponding to (1, 3) or (3, 1). For simplicity, the single descriptor (1, 3) is to be applied to both the latter cases. There are 24 different time-orderings for the type exemplified in Fig. 5(a), as well as “mirror-image” counterparts exchanging the roles of the two emitters A and B for each of the possibilities exemplified in Fig. 5(b), giving a total of 72 different time-orderings that must all be taken into account. A similar pattern arises in the theory of laser-induced energy transfer.³⁴

The two forms of coupling represented in Fig. 5 are not necessarily of equal significance. The case illustrated in Fig. 5(a), for example, requires that the electronic decay transition $0 \leftarrow m$ satisfies two-photon ($E1^2$) selection rules, whereas Fig. 5(b) is supported only when the given transition, since it occurs in both particles, must satisfy both one- and three-photon criteria ($E1$ and $E1^3$). If the emitters have a centrosymmetric structure, then each electronic state must be of either *gerade* (g) or *ungerade* (u) symmetry and it is obviously not possible for both mechanisms to be simultaneously operative: one will be allowed and the other forbidden. Other symmetry elements will also lead to instances of mutual exclusion, depending on the symmetry class and the irreducible representations of the relevant electronic states. A thorough discussion of the selection rules for (2, 2) and (1, 3) coupling, including a full listing of the transitions allowed for each representation of all the major point groups, can be found in earlier work on bimolecular optical absorption.³⁵

We now proceed with the QED analysis. Here, in view of the considerably higher level of complexity that arises in this case, a retarded coupling method devised by Dávila Romero and Andrews is deployed.³⁶ To base analysis on this method it suffices to consider only one time-ordered diagram for each set of photonic interactions, expediently focusing on the types that in each successive interaction adhere most closely to energy conservation—which are those depicted in Fig. 5. This method gives the matrix element for the coupling between

each of N molecules, labeled ξ_i , as

$$M_{fi} = R_{rad} \times \text{Re} \left[\tilde{\chi}_{\{k_1\}}^{\xi_1} \times \prod_{j=2}^N V_{\{k_j\}\{k_{j+1}\}}(k, \mathbf{R}_{\xi_{j+1}\xi_j}) \times \tilde{\chi}_{\{k_1\}}^{\xi_1} \right]. \quad (34)$$

Here, R_{rad} is a scalar factor relating to the change in radiation state, its precise form dictated by a specific prescription; so too is the argument k of the retarded coupling tensor;³⁶ $\mathbf{R}_{\xi_{j+1}\xi_j}$ denotes the vector separation between each of the particles, and $\tilde{\chi}_{\{k_1\}}^{\xi_1}$ is an interaction tensor whose Cartesian index

set $\{k_i\}$ is determined by the number of photon events at the corresponding particle. The tensor $\tilde{\chi}_{\{k_1\}}^{\xi_1}$ in its general form is a nonlinear polarizability contracted with polarization vectors for the photons.³⁷ This method circumvents a lengthy addition of matrix element contributions associated with the multiplicity of time-orderings.

The complete set of interactions of the (2, 2) type illustrated in Fig. 5(a) involves one real and one virtual photon interaction at each particle, giving both $\tilde{\chi}_{\{k_1\}}^{\xi_1}$ and $\tilde{\chi}_{\{k_2\}}^{\xi_2}$ as generalized forms of the polarizability tensor $\alpha_{ij}(\omega) \equiv \alpha_{ij}(-ck; ck)$ from Eq. (22).¹³ Explicitly, the calculation gives

$$M_{fi}^{(\alpha,\alpha)} = \left(\frac{\hbar ck_1}{2\epsilon_0 V} \right)^{1/2} \left(\frac{\hbar ck_2}{2\epsilon_0 V} \right)^{1/2} \bar{e}_i^{(\eta)}(\mathbf{k}_1) \alpha_{ij}^{0m(A)}(ck_1 - ck; -ck_1) \\ \times V_{jk}(-k_1 + k, \mathbf{R}) \alpha_{kl}^{0m(B)}(-ck_2; ck_2 - ck) \bar{e}_l^{(\eta')}(\mathbf{k}_2) e^{-i\mathbf{k}_1 \cdot \mathbf{R}} + [k_1 \leftrightarrow k_2], \quad (35)$$

where

$$\alpha_{ij}^{xy(\xi)}(\pm ck', \pm ck) = \sum_s \left[\frac{\mu_i^{xs(\xi)} \mu_j^{sy(\xi)}}{E_{sy}^{(\xi)} \mp \hbar ck'} + \frac{\mu_j^{xs(\xi)} \mu_i^{sy(\xi)}}{E_{sy}^{(\xi)} \mp \hbar ck} \right]. \quad (36)$$

Now in summing over all possible frequency pairs for the two emitted photons, the matrix element (35) is weighted towards the contribution where $k_1 = k_2$; this makes physical sense and is borne out by the product $k_1 k_2$ included at the front of that equation. In consequence the corresponding rate result will be dominated by terms in which the $(k - k_1)$ wave-number argument of the V tensor is close to zero, signifying quasi-static coupling.

The (1, 3) mechanism, as seen from the example time-ordering shown in Fig. 5(b), involves one virtual photon interaction at each particle and two real photon interactions at one of them. The particle with a single interaction will undergo decay mediated by a transition dipole—the decay of the other particle with three interactions, a transition hyperpolarizability. These two tensors are connected by the retarded potential tensor of Eq. (24),

$$M_{fi}^{(\mu,\beta)} = \left(\frac{\hbar ck_1}{2\epsilon_0 V} \right)^{1/2} \left(\frac{\hbar ck_2}{2\epsilon_0 V} \right)^{1/2} [\bar{e}_i^{(\eta)}(\mathbf{k}_1) \bar{e}_j^{(\eta')}(\mathbf{k}_2) \beta_{ijk}^{0m(B)}(-ck_1, -ck_2, ck) V_{kl}(k, \mathbf{R}) \mu_l^{0m(A)} e^{-i(k_1+k_2) \cdot \mathbf{R}} \\ + \bar{e}_i^{(\eta)}(\mathbf{k}_1) \bar{e}_j^{(\eta')}(\mathbf{k}_2) \beta_{ijk}^{0m(A)}(-ck_1, -ck_2, ck) V_{kl}(k, \mathbf{R}) \mu_l^{0m(B)}], \quad (37)$$

where the second term, secured on exchanging the roles of A with B , carries no phase factor because both photons are emitted from the coordinate origin located at A . In passing we note that the coupling tensor V is symmetric with respect to the sign of vector \mathbf{R} , simplifying the following analysis. The generalized hyperpolarizability tensor in (37) is explicitly given by the following sum-over-states formula:

$$\beta_{jkl}^{mn(\xi)}(ck'', ck', ck) = \sum_{s,r} \left\{ \frac{\mu_j^{ms(\xi)} \mu_k^{sr(\xi)} \mu_l^{rn(\xi)}}{(E_{sn}^{(\xi)} - \hbar ck' - \hbar ck)(E_{rn}^{(\xi)} - \hbar ck)} + \frac{\mu_j^{ms(\xi)} \mu_l^{sr(\xi)} \mu_k^{rn(\xi)}}{(E_{sn}^{(\xi)} - \hbar ck' - \hbar ck)(E_{rn}^{(\xi)} - \hbar ck')} \right. \\ + \frac{\mu_k^{ms(\xi)} \mu_j^{sr(\xi)} \mu_l^{rn(\xi)}}{(E_{sn}^{(\xi)} - \hbar ck'' - \hbar ck)(E_{rn}^{(\xi)} - \hbar ck)} + \frac{\mu_k^{ms(\xi)} \mu_l^{sr(\xi)} \mu_j^{rn(\xi)}}{(E_{sn}^{(\xi)} - \hbar ck'' - \hbar ck)(E_{rn}^{(\xi)} - \hbar ck'')} \\ \left. + \frac{\mu_l^{ms(\xi)} \mu_j^{sr(\xi)} \mu_k^{rn(\xi)}}{(E_{sn}^{(\xi)} - \hbar ck'' - \hbar ck')(E_{rn}^{(\xi)} - \hbar ck')} + \frac{\mu_l^{ms(\xi)} \mu_k^{sr(\xi)} \mu_j^{rn(\xi)}}{(E_{sn}^{(\xi)} - \hbar ck'' - \hbar ck')(E_{rn}^{(\xi)} - \hbar ck'')} \right\}. \quad (38)$$

Again, the result (37) can be simplified on the assumption that both emitters have a common orientation, so that the two terms it comprises become equal, save for the phase factor.

To secure the rate of correlated emission, we deploy the Fermi rule, Eq. (2), in which the appropriate density of radiation states ρ_{AB} is here given by a convolution of the density of states for each emission mode:

$$\rho_{AB} = \hbar c \int \rho(k_1) \rho(2k - k_1) dk_1 \quad (39)$$

with k_2 expressed in terms of k_1 , by virtue of energy conservation. The integral in (39) is to be effected over the range (0, $2k$), resulting in the following number of radiation states per unit energy interval, and per unit solid angle in each of the two emission directions:

$$\rho_{AB} = \frac{k^5}{60\pi^6 \hbar c} V^2. \quad (40)$$

At this juncture, to keep a focus on the key physical features, we shall simplify the analysis by assuming that each emission is allowed by E1 (and E1³) selection rules, but forbidden for E1²—the latter condition being a corollary of the former assumption, in the case of centrosymmetric species. For this reason, we therefore limit consideration to the (1, 3) mechanism, which is satisfied by most systems whose initial excitation is of E1 form. The more general case where the decay is simultaneously E1, E1² and E1³ allowed follows along similar lines; the general expression just contains many more terms. The total rate of two-photon emission is now given by

$$\begin{aligned} \Gamma^{(\mu,\beta)} &= \left(\frac{\pi \hbar c^2 k_1 k_2}{2 \varepsilon_0^2 V^2} \right) [\bar{e}_i^{(\eta)}(\mathbf{k}_1) e_m^{(\eta)}(\mathbf{k}_1) \bar{e}_j^{(\eta)}(\mathbf{k}_2) e_n^{(\eta)}(\mathbf{k}_2) \\ &\times (2 + e^{-i(k_1+k_2) \cdot R} + e^{i(k_1+k_2) \cdot R}) \times \beta_{ijk}^{0m} \\ &\times \beta_{mno}^{0m} V_{kl}(k, \mathbf{R}) \bar{V}_{op}(k, \mathbf{R}) \mu_l^{0m} \mu_p^{0m}] \rho_{AB}. \end{aligned} \quad (41)$$

Independent summations need to be performed over the polarizations of the two emitted photons; for each, we can use the result given in Sec. III A. Hence, using the density of radiation states (40), we find

$$\begin{aligned} \Gamma^{(\mu,\beta)} &= \text{Re} \left(\frac{ck^5 k_1 k_2}{60\pi^5 \varepsilon_0^2} \right) V_{kl}(k, \mathbf{R}) \bar{V}_{op}(k, \mathbf{R}) \mu_l^{0m} \mu_p^{0m} \left[\beta_{ijk}^{0m} \beta_{ijo}^{0m} \right. \\ &+ \left(\frac{1}{k_1^3 k_2^3 R^6} \right) (\beta_{ijk}^{0m} \beta_{mno}^{0m} \hat{R}_i \hat{R}_m \hat{R}_j \hat{R}_n \\ &- \frac{2}{3} \beta_{ijk}^{0m} \beta_{mjo}^{0m} \hat{R}_i \hat{R}_m + \frac{1}{9} \beta_{ijk}^{0m} \beta_{ijo}^{0m}) \\ &\times (3 \sin k_1 R - 3k_1 R \cos k_1 R - k_1^2 R^2 \sin k_1 R) \\ &\left. \times (3 \sin k_2 R - 3k_2 R \cos k_2 R - k_2^2 R^2 \sin k_2 R) \right] \end{aligned} \quad (42)$$

using the index symmetry between the first two indices of the hyperpolarizability tensor. Once again we observe that the result is dominated by the case $k_1 = k_2 = k$, and on taking the

limit $kR \gg 1$, the following result is obtained:

$$\begin{aligned} \Gamma^{(\mu,\beta)} &= \left(\frac{ck^{11}}{960\pi^7 \varepsilon_0^4 R^2} \right) \mu_l^{0m} \mu_p^{0m} (\delta_{kl} - \hat{R}_k \hat{R}_l) \\ &\times (\delta_{op} - \hat{R}_o \hat{R}_p) \left[\beta_{ijk}^{0m} \beta_{ijo}^{0m} \right. \\ &+ \left(\frac{1}{9k^2 R^2} \right) (9\beta_{ijk}^{0m} \beta_{mno}^{0m} \hat{R}_i \hat{R}_m \hat{R}_j \hat{R}_n \\ &\left. - 6\beta_{ijk}^{0m} \beta_{mjo}^{0m} \hat{R}_i \hat{R}_m + \beta_{ijk}^{0m} \beta_{ijo}^{0m}) \sin^2 kR \right] \end{aligned} \quad (43)$$

the result displaying a non-oscillatory R^{-2} distance-decay term, tempered by an R^{-4} oscillatory term that runs as $\sin^2 kR$. The spatial frequency of the latter oscillation is once again twice that of the experimental result. In contrast to the coupled result of Sec. III B, terms in the above result involving components of \mathbf{R} do not necessarily vanish in the case where the transition moments are disposed orthogonally to the pair separation, because here the corresponding index contractions engage the hyperpolarizability tensors. As before, we reserve further discussion for Sec. IV, where all three cases are assessed in the same context; this concludes our derivation of the rate equations for the three key mechanisms of pair decay.

IV. DISCUSSION

Using the tools of quantum electrodynamics, we have set forth a comprehensive survey of three mechanisms that can produce distinctive pair-coupling features in spontaneous optical emission. Since the initial states differ in each of the described mechanisms, there is no question of competition or quantum interference taking place between them; they can be regarded as entirely separate. Each of the processes is characterized by a unique form of rate equation, providing reasonable grounds for experimentally distinguishing between them. As we have shown, the reported fit of data from the pioneering experimental work¹² that prompted our study in fact shows no evidence of electrodynamic coupling between the emitters, surprisingly at odds with the original conclusions.

First, analysis of the emission from a symmetric exciton state has revealed the observed modification of the pair emission rate, compared to that of an isolated emitter—the result given in Eq. (18), when $kR \gg 1$ —displays a position-dependence running as $R^{-1} \sin kR$. Although broadly agreeing with the reported form of experimental data, including a damped oscillation with a cycle roughly equal to the emission wavelength, this does not signify electrodynamic coupling between the emitters. All that is required is for static coupling to support frequency-shifted combination states; the result can be interpreted as revealing quantum mechanical interference between emission at two separate sites. Moreover, a superposition of the symmetric and antisymmetric exciton states will clearly produce no change from the free emission rate. Any observations of an emission rate with a damped oscillatory dependence on the pair separation, due to this interference mechanism, would therefore require a sufficient lifting of degeneracy that only one of the exciton states is initially

excited. Also, similarly separation-dependent oscillations in rate, but displaying the opposite spatial phase, might then be anticipated where emission from the antisymmetric combination occurs.

Our second calculation determined the rate of emission associated with the single-photon fluorescence of a pair, the general result of Eq. (32) accommodating full electrodynamic coupling. This is a case where quantum mechanical interference occurs between the amplitudes associated with two different orders of perturbation theory. One immediate difference from the exciton case is that this result engages the electronic polarizability α , which favors the coupling mechanism for emitters that are highly polarizable—as indeed is the case with the extensively electronically delocalized polymer materials used in the first experiments. Proceeding to secure a general rate equation, applicable over all pair separation distances, our analysis has then once again focused on a result for the scale $kR \gg 1$, identifying a dominant distance characteristic of $R^{-2} \sin 2kR$ form. On this basis, the result from Barnes *et al.* appears more consistent with the lower spatial frequency modulation of the exciton result.

The third mechanism is primarily distinguished by a decay releasing two photons, rather than one, from the nanoantenna pair. As we have shown, the necessary initial condition correspondingly requires both emitters to be simultaneously excited—and although this is not unrealistic, it is undoubtedly a more demanding criterion than applies to the other two cases. One notable feature of this mechanism is that no quantum interference is involved. Our analysis has revealed that two distinct variants of this mechanism can occur, but that since each is subject to different symmetry selection rules, one involving the hyperpolarizability would commonly dominate. With this specific mechanism whose general result is given in Eq. (42) (and also in the case where two polarizabilities are coupled), far-field distance modulation of the emission rate takes the form of $R^{-4} \sin^2 kR$, the oscillations occurring with the same doubling of spatial frequency that arises with the second mechanism.

There is a wide range of physical systems within which pair emission phenomena can prove significant. For example, it is well known that mutual coherence and interference can be exhibited by a simple pair of atoms, free or coupled to an optical cavity mode.^{38,39} The recent advances in theory in this area^{5-7,32,40,41} further indicate the broad scope for the experimental characterization of pair emission effects in a variety of physically different media. With the benefit of the details we have provided, it should now be possible to design experiments to specifically target one or other mechanism, and to verify (or challenge) the form of distance dependence that we have identified in each case. Our work also paves the way for wider extensions of these principles; the next challenge is to investigate the effects of pair-wise coupling between components in regular geometric arrays of molecular emitters.

Concluding with an example at the opposite extreme of molecular complexity, it is interesting to note increasing recognition of the important role played by coupled antenna molecules in a number of photosynthetic systems—notably the Fenna-Matthews-Olson (FMO) complex in green sulfur bacteria. It is now understood that exciton delocalization and

coherence in such systems, following the initial absorption of light, can substantially modify the ensuing mechanisms of energy transfer.⁴²⁻⁴⁴ Indeed the results of several studies based on two-dimensional laser spectroscopy are almost incomprehensible if quantum coherence is not taken into account.^{45,46} As the theory for such complex systems is more fully elucidated, it will be necessary for experimentalists to carefully discriminate between the various mechanisms for fluorescence and energy transfer, that can operate when a single excitation is shared between chromophores. In this connection, too, we hope that the present study might contribute additional insight.

ACKNOWLEDGMENTS

We are most grateful for numerous helpful comments on the manuscript, from David Bradshaw and Matt Coles. This research was funded by the University of East Anglia.

APPENDIX: VIRTUAL PHOTON MODE SUM

Collecting all p -dependent terms in (21) gives

$$\frac{1}{2\varepsilon_0 V} \sum_{p, \eta'} p \bar{e}_i^{(\eta')}(\mathbf{p}) e_j^{(\eta')}(\mathbf{p}) \left\{ \frac{e^{i\mathbf{p}\cdot\mathbf{R}}}{(p-k)} + \frac{e^{-i\mathbf{p}\cdot\mathbf{R}}}{(p+k)} \right\} \quad (\text{A1})$$

and the polarization sum is given by (14). For large V the p -sum converts to an integral,

$$\lim_{V \rightarrow \infty} \frac{1}{V} \sum_{\mathbf{p}} \equiv \int \frac{d^3 \mathbf{p}}{(2\pi)^3}. \quad (\text{A2})$$

Using

$$(\delta_{ij} - \hat{p}_i \hat{p}_j) e^{\pm i\mathbf{p}\cdot\mathbf{R}} = (-\nabla^2 \delta_{ij} + \nabla_i \nabla_j) \frac{1}{p^2} e^{\pm i\mathbf{p}\cdot\mathbf{R}} \quad (\text{A3})$$

and with angular integration, (21), we find the principal value for the matrix element

$$M_{fi}^{P,V} = -i \left(\frac{\hbar ck}{2\varepsilon_0 V} \right)^{1/2} e_k^{(\eta)}(\mathbf{k}) e^{-i\mathbf{k}\cdot\mathbf{R}} \mu_i^{0m}(A) \alpha_{jk}^B(\omega) \\ \times \frac{1}{4\pi \varepsilon_0} (-\nabla^2 \delta_{ij} + \nabla_i \nabla_j) \frac{\cos kR}{R}. \quad (\text{A4})$$

The poles from graphs (a) and (b) of Fig. 3, where the virtual photon energy equals the transition energy, are dealt with using the standard infinitesimal imaginary addendum ε ,

$$\frac{1}{x-a \pm i\varepsilon} = \frac{P}{x-a} \mp i\pi \delta(x-a). \quad (\text{A5})$$

The second term on the right, the delta function contribution from the poles, after summing over all polarizations and again converting the p -sum to an integral, is then

$$\begin{aligned}
M_{fi}^{\delta} &= - \sum_r i \left(\frac{\hbar ck}{2\epsilon_0 V} \right)^{1/2} \int \frac{\hbar cp}{2\epsilon_0} (\delta_{ij} - \hat{p}_i \hat{p}_j) e_k^{(\eta)}(\mathbf{k}) e^{-i\mathbf{k}\cdot\mathbf{R}} \mu_i^{0m}(A) \mu_j^{r0}(B) \mu_k^{0r}(B) \\
&\quad \times e^{i\mathbf{p}\cdot\mathbf{R}} i\pi \delta(\hbar cp - E_m^A) \left(\frac{1}{E_{r0}^B - E_{m0}^A} + \frac{1}{E_{r0}^B + \hbar cp} \right) \frac{d^3 \mathbf{p}}{(2\pi)^3} \\
&= i \left(\frac{\hbar ck}{2\epsilon_0 V} \right)^{1/2} e_k^{(\eta)}(\mathbf{k}) e^{-i\mathbf{k}\cdot\mathbf{R}} \mu_i^{0m}(A) \alpha_{jk}^B(\omega_{m0}) \frac{1}{4\pi\epsilon_0} (-\nabla^2 \delta_{ij} + \nabla_i \nabla_j) \frac{i \sin kR}{R}.
\end{aligned} \tag{A6}$$

Adding to the principal value (A4) gives the following complete third order matrix element:

$$\begin{aligned}
M_{fi}^{(3)} &= -i \left(\frac{\hbar ck}{2\epsilon_0 V} \right)^{1/2} \bar{e}_k^{(\eta)}(\mathbf{k}) e^{-i\mathbf{k}\cdot\mathbf{R}} \mu_i^{0m}(A) \alpha_{jk}^B(\omega) \frac{1}{4\pi\epsilon_0} \\
&\quad \times (-\nabla^2 \delta_{ij} + \nabla_i \nabla_j) \frac{e^{ikR}}{R}.
\end{aligned} \tag{A7}$$

¹Optical Properties of Nanostructured Random Media, Topics in Applied Physics Vol. 82, edited by V. M. Shalaev (Springer, Berlin, 2002).

²W. L. Barnes, A. Dereux, and T. W. Ebbesen, "Surface plasmon subwavelength optics," *Nature (London)* **424**, 824–830 (2003).

³S. Lal, S. Link, and N. J. Halas, "Nano-optics from sensing to waveguiding," *Nat. Photon.* **1**, 641–648 (2007).

⁴A. E. Miroshnichenko, I. S. Maksymov, A. R. Davoyan, C. Simovski, P. Belov, and Y. S. Kivshar, "An arrayed nanoantenna for broadband light emission and detection," *Phys. Status Solidi: Rapid Res. Lett.* **5**, 347–349 (2011).

⁵S. I. Schmid and J. Evers, "Interplay of vacuum-mediated inter- and intra-atomic couplings in a pair of atoms," *Phys. Rev. A* **81**, 063805 (2010).

⁶J. Evers, M. Kiffner, M. Macovei, and C. H. Keitel, "Geometry-dependent dynamics of two Λ -type atoms via vacuum-induced coherences," *Phys. Rev. A* **73**, 023804 (2006).

⁷S. I. Schmid and J. Evers, "Dipole-dipole interaction between orthogonal dipole moments in time-dependent geometries," *Phys. Rev. A* **77**, 013822 (2008).

⁸R. Corkish, M. A. Green, and T. Puzzer, "Solar energy collection by antennas," *Solar Energy* **73**, 395–401 (2002).

⁹D. R. Ward, F. Hüser, F. Pauly, J. C. Cuevas, and D. Natelson, "Optical rectification and field enhancement in a plasmonic nanogap," *Nat. Nanotechnol.* **5**, 732–736 (2010).

¹⁰L. Novotny and N. van Hulst, "Antennas for light," *Nat. Photon.* **5**, 83–90 (2011).

¹¹T.-H. Lee, P. Kumar, A. Mehta, K. Xu, R. M. Dickson and M. D. Barnes, "Oriented semiconducting polymer nanostructures as on-demand room-temperature single-photon sources," *Appl. Phys. Lett.* **85**, 100 (2004).

¹²M. D. Barnes, P. S. Krstic, P. Kumar, A. Mehta, and J. C. Wells, "Far-field modulation of fluorescence decay rates in pairs of oriented semiconducting polymer nanostructures," *Phys. Rev. B* **71**, 241303 (2005).

¹³D. P. Craig and T. Thirunamachandran, *Molecular Quantum Electrodynamics. An Introduction to Radiation-Molecule Interactions* (Dover, New York, 1998).

¹⁴A. Salam, *Molecular Quantum Electrodynamics. Long-Range Intermolecular Interactions* (Wiley, Hoboken, NJ, 2010).

¹⁵G. Grynberg, A. Aspect, and C. Fabre, *Introduction to Quantum Optics. From the Semi-Classical Approach to Quantized Light* (Cambridge University Press, Cambridge, 2010), Sect. 5.2.2.

¹⁶D. L. Andrews and D. S. Bradshaw, "Virtual photons, dipole fields and energy transfer: a quantum electrodynamical approach," *Eur. J. Phys.* **25**, 845–858 (2004).

¹⁷R. G. Woolley, "Charged particles, gauge invariance, and molecular electrodynamics," *Int. J. Quantum Chem.* **74**, 531–545 (1999).

¹⁸D. L. Andrews and G. Juzeliūnas, "Intermolecular energy transfer: Retardation effects," *J. Chem. Phys.* **96**, 6606–6612 (1992).

¹⁹G. J. Daniels, R. D. Jenkins, D. S. Bradshaw, and D. L. Andrews, "Resonance energy transfer: The unified theory revisited," *J. Chem. Phys.* **119**, 2264–2274 (2003).

²⁰D. L. Andrews, C. Curutchet, and G. D. Scholes, "Resonance energy transfer: beyond the limits," *Laser Photon. Rev.* **5**, 114–123 (2011).

²¹M. O. Scully and M. S. Zubairy, *Quantum Optics* (Cambridge University Press, Cambridge, 1997), Sect. 1.5.2.

²²S. V. Gaponenko, *Introduction to Nanophotonics* (Cambridge University Press, Cambridge, 2010), Sect. 13.5.

²³D. P. Craig and T. Thirunamachandran, "Radiation-molecule and molecule-molecule interactions. A unified viewpoint from quantum electrodynamics," *Acc. Chem. Res.* **19**, 10–16 (1986).

²⁴D. P. Craig and T. Thirunamachandran, "The influence of intermolecular coupling on spontaneous emission," *Mol. Phys.* **88**, 631–645 (1996).

²⁵E. M. Rice, D. S. Bradshaw, K. Saadi and D. L. Andrews, "Identifying the development in phase and amplitude of dipole and multipole radiation," *Eur. J. Phys.* **33**, 345–358 (2012).

²⁶M. Kasha, H. R. Rawls and M. Ashraf El-Bayoumi, "The exciton model in molecular spectroscopy," *Pure Appl. Chem.* **11**, 371–592 (1965).

²⁷E. A. Power and T. Thirunamachandran, "Quantum electrodynamics with non relativistic sources. III. Intermolecular interactions," *Phys. Rev. A* **28**, 2671–2675 (1983).

²⁸E. A. Power, *Introductory Quantum Electrodynamics* (Longman, London, 1964).

²⁹A. Salam, "A general formula for the rate of resonant transfer of energy between two electric multipole moments of arbitrary order using molecular quantum electrodynamics," *J. Chem. Phys.* **122**, 044112 (2005).

³⁰A. Salam, "Resonant transfer of excitation between two molecules using Maxwell fields," *J. Chem. Phys.* **122**, 044113 (2005).

³¹D. L. Andrews and M. J. Harlow, "Phased and Boltzmann-weighted rotational averages," *Phys. Rev. A* **29**, 2796–2806 (1984).

³²P. R. Berman, "Spontaneous emission and scattering in a two-atom system: conservation of probability and energy," *Phys. Rev. A* **76**, 043816 (2007).

³³Y. Ota, S. Iwamoto, N. Kumagai, and Y. Arakawa, "Spontaneous two-photon emission from a single quantum dot," *Phys. Rev. Lett.* **107**, 233602 (2011).

³⁴P. Allcock, R. D. Jenkins, and D. L. Andrews, "Laser assisted resonance energy transfer," *Chem. Phys. Lett.* **301**, 228–234 (1999).

³⁵D. L. Andrews and A. M. Bittner, "Selection rules for bimolecular photoabsorption," *Chem. Phys.* **165**, 1–10 (1992).

³⁶L. C. Dávila Romero and D. L. Andrews, "A retarded coupling approach to intermolecular interactions," *J. Phys. B: At. Mol. Opt. Phys.* **42**, 085403 (2009).

³⁷D. S. Bradshaw and D. L. Andrews, "Optically controlled resonance energy transfer: Mechanism and configuration for all-optical switching," *J. Chem. Phys.* **128**, 144506 (2008).

³⁸J. W. Czarnik and P. R. Fontana, "Resonance radiation from interacting atoms," *J. Chem. Phys.* **50**, 4071–4074 (1969).

³⁹P. Kochan, H. J. Carmichael, P. R. Morrow, and M. G. Raizen, "Mutual coherence and interference in resonance fluorescence," *Phys. Rev. Lett.* **75**, 45–48 (1995).

⁴⁰G.-P. Cheng, S.-S. Ke, L.-H. Zhang, and G.-X. Li, "The coherence of resonance fluorescence for two atoms in a cavity," *Acta Phys. Sin.* **56**, 830–836 (2007).

- ⁴¹J. Luling, N. Yueping, and G. Shangqing, "Phase control of spatial interference from two duplicated two-level atoms," *Phys. Rev. A* **83**, 023410 (2011).
- ⁴²J. Adolphs and T. Renger, "How proteins trigger excitation energy transfer in the FMO complex of green sulfur bacteria," *Biophys. J.* **91**, 2778–2797 (2006).
- ⁴³A. Ishizaki and G. R. Fleming, "Unified treatment of quantum coherent and incoherent hopping dynamics in electronic energy transfer: Reduced hierarchy equation approach," *J. Chem. Phys.* **130**, 234111 (2009).
- ⁴⁴B. Cui, X. X. Yi, and C. H. Oh, "Excitation energy transfer in light-harvesting systems: effect of the initial state," *J. Phys. B: At. Mol. Opt. Phys.* **45**, 085501 (2012).
- ⁴⁵Y.-C. Cheng and G. R. Fleming, "Dynamics of light-harvesting in photosynthesis," *Annu. Rev. Phys. Chem.* **60**, 241–262 (2009).
- ⁴⁶J. R. Caram, N. H. C. Lewis, A. F. Fidler, and G. S. Engel, "Signatures of correlated excitonic dynamics in two-dimensional spectroscopy of the Fenna-Matthew-Olson photosynthetic complex," *J. Chem. Phys.* **136**, 104505 (2012).